Renewable Energy 256 (2026) 123942

Contents lists available at ScienceDirect

Renewable Energy

journal homepage: www.elsevier.com/locate/renene

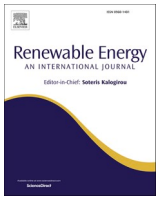

Is an exact backside irradiance modelling essential for bifacial PV systems?

Kristijan Brecl [a,*], Emilio Muñoz Cerón [b], Juan de la Casa Higueras [b], Marko Topič [a]

[a] LPVO, Faculty of Electrical Engineering, University of Ljubljana, Tržaška 25, SI-1000, Ljubljana, Slovenia
[b] PV IDEA Research Group, Centre for Advanced Studies in Earth Science, Energy and Environment, University of Jaén, Spain

ARTICLE INFO

Keywords:
PV systems
Backside irradiance
Modelling
Energy yield

ABSTRACT

Backside irradiance modelling for photovoltaic (PV) modules is not simple and straightforward as it highly depends on the situation of an actual system. In addition, the irradiance conditions can change from one side of a PV system to the other due to the reflections from the ground or surroundings. Currently, all available models are based on analytical methods. Here, we present a new empirical model for backside irradiance for fixed PV systems modelled by a Gaussian function on the backside irradiance share and compare the results with an analytical model. Furthermore, we have applied different backside irradiance calculations to a PV performance rating model and compared the results. Our calculations, verified with the data from three different locations in Europe, have shown that for common PV systems, where the backside irradiance share is relatively low, annual PV performance calculations can be performed with a fixed backside irradiance share value.

1. Introduction

In recent years, bifacial crystalline silicon solar cells have been the leading technology in the photovoltaic (PV) market. By the end of 2024, 90% of all fabricated silicon-based solar cells were already bifacial. Similarly, more than 60% of the module market is expected to use bifacial PV modules in the following years, with an additional 30% of monofacial PV modules incorporating bifacial solar cells [1]. Although bifacial cells require additional manufacturing steps, such as the backside texturing and AR coating, they enable a significant reduction in the metal consumption for the electrical contacts. As a result, bifacial PV modules are now widely used in various applications, including open-rack systems, rooftop and even in integrated PV systems.

The bifacial cells in monofacial PV modules can benefit from internal reflections from the backsheet [2], but the main benefit can be achieved in open-rack systems where direct or reflected sunlight can reach the cell from both sides. To achieve this, bifacial PV modules require a glass/-glass or, in some cases, a glass/transparent backsheet structure that allows light also to enter the cell from the rear side. To minimise back shading, junction boxes at the back side are moved to the sides or centre of the module to ensure they do not cover the surface of a cell and block light from reaching the cell.

The widespread use of bifacial solar cells in both monofacial and bifacial PV modules raises the question whether the current standard measurement procedures under standard test conditions (STC), which are primarily designed for direct light, and energy rating models are still good enough. There is a need to analyse whether such standardized conditions need to be adapted for bifacial modules. A technical specification for the measurement of current-voltage characteristics, published in 2019 [3], describes recommendations for the correct measurement of the output power of a bifacial PV module.

However, given the aforementioned variety of configurations in which bifacial PV modules are used, the adequacy of existing energy rating models remains uncertain.

The main challenge is to accurately model the backside irradiance, which varies significantly depending on the environmental conditions and system configurations. Currently, the backside irradiance is modelled using sky- and ground-view factors, calculated by using the solar and PV system geometry or by ray tracing models.

Vogt et al. [4] propose to define the backside irradiance according to the IEC 61853-3 standard [5] for energy estimation. Several researchers have published energy assessment models that analytically simulate the backside irradiance based on the geometry of the sun's position and the PV system. Yusufoglu et al. [6] treated the backside irradiance as a ground-reflected light using the sky-view factor principle. The same approach, where the ground reflected light is reduced by the self-shading of the module, is used in Ref. [7]. Ground view factor calculations influenced by module shading are used also by Ref. [8]. Wang et al. [9] use solar geometry to calculate the ground reflected light and backside irradiance. At Sandia National Laboratories a true geometric

* Corresponding author.
E-mail address: kristijan.brecl@fe.uni-lj.si (K. Brecl).

https://doi.org/10.1016/j.renene.2025.123942
Received 6 May 2025; Received in revised form 19 June 2025; Accepted 5 July 2025
Available online 8 July 2025

model for backside irradiance was developed [10], using both the geometry of the sun and the geometry of the PV system to accurately calculate backside irradiance. A step further was taken by Valdivia et al. [11], where a ray tracing model was used to simulate the backside irradiance.

Common to all models is that they need information about the geometry of the PV system and often require a lot of computational power. Models based on view factors can reliably estimate the backside irradiance, particularly when the front irradiance used in the calculations has been measured. However, they cannot account for reflections from the modules in the back row or the mounting frames. Models using view factors require only basic geometric data on the PV system, such as the inclination angle and height, and ground albedo values. In contrast, geometric and ray tracing models require more precise information about the supporting structure's geometry. Additionally, they can include albedo and reflectivity from all surrounding surfaces, resulting in a higher accuracy, but they are also more complex and computationally time-consuming.

Due to the limitations of the currently available models, we looked for an empirical model that could be used universally. Empirical models have the benefit of including all the local effects that cannot be foreseen in an analytical model, but they can deviate in the accuracy throughout the year and at different irradiance levels if only one fitting curve is used. While an empirical model does not require PV system geometry, it does require backside irradiance measurements during the training period.

Bouchakour et al. [12] applied performance models developed for monofacial modules to estimate the energy yield of bifacial PV modules and found that analytical models outperform the empirical models. Recently, we reported an energy rating model for bifacial PV modules where the backside irradiance was defined from the average measured annual share of the backside irradiance [13].

A persistent problem in all energy rating models for bifacial PV modules is the accurate definition and modelling of the backside irradiance. In this paper, we address the challenges of modelling backside irradiance for fixed PV systems, the limitations of both analytical and empirical models, and the performance of a new empirical model for backside irradiance.

The paper is divided into three main sections. In the first part the challenges of backside irradiance modelling are discussed, focusing on measurement issues and non-uniformity. Next, a new empirical model for backside irradiance is presented and its performance compared to an analytical model. Finally, the simulated irradiance is used to calculate PV system performance indicators. The objective of this paper is to assess the importance of backside irradiance modelling in the calculation of bifacial PV system performance indicators, with the specific aim of determining whether such modelling is essential for an accurate evaluation. This question is addressed and discussed in detail in the conclusions of the paper.

2. Backside irradiance modelling: situation, issues and models

Nowadays, solar irradiance models are well developed with both, analytical and heuristic approaches providing reliable simulations of clear-sky global horizontal irradiance (GHI) with reasonable accuracy. The first broadband model dates back to the 1960s, i.e. ASHRAE [14], followed by widely used models such as Bird [15] and, Ineichen [16], among others. A comprehensive comparison of these models has been published by Gueymard [17]. Analytical cloudy-sky models were published by Kasten et al. [18] and Badescu [19].

In the recent years, the popularity of analytical models has declined, as energy performance assessment models are now based on measured, satellite-derived data (SARAH [20] and CLARA-A2 [21]) or reanalysed datasets such as ERA5 or CAMS [22]. Plane-of-array irradiance is typically calculated using transposition models like mostly cited Perez model [23] or Hay model [24].

While these models can adequately simulate front and back irradiance for vertically mounted modules, challenges arise for tilted modules, where backside irradiance is dominated by reflected light. Conventional models may fail to meet the accuracy requirements for backside irradiance under these conditions. The backside obstruction, seasonality of reflectivity and the non-uniformity of the light reflected from the ground are the key issues in calculating backside irradiance thus new models for backside irradiance have to be developed. The following subsections describe the specific conditions for backside irradiance modelling.

2.1. Location and mounting situation

The location and, in particular, the mounting structure have a major impact on the backside irradiance. Therefore, bifacial PV systems require special support structures that ideally do not cover the cells from behind. However, in practice, support rails are required to ensure the stability and resistance in all weather conditions (Fig. 1). The distance between the module and the support elements can have a direct effect on the shading of the back of the PV modules; closer rails produce sharper shadows.

Ground clearance is another critical factor, as it affects the module's own shading and, consequently, the reflected irradiance. Fig. 1 clearly shows how the proportion of the visible ground that is shaded varies depending on the distance of the module above the ground.

2.2. Partial shading and non-uniform illumination

In addition to the modules' self-shading, support elements such as aluminium rods near the cells (see picture on Fig. 1 – left) do not only partially shade the cells, but also cause a reflection. Consequently, a single cell may experience three conditions: "normal" back side irradiance (marked as "G" in Fig. 2), enhanced irradiance from reflections ("G+" in Fig. 2) and reduced irradiance due to shading ("G-" in Fig. 2).

While frontside shading can have a large impact on the module output power and can even lead to reverse bias on the shaded cell, backside irradiance variations are less critical and cannot lead to a reverse bias on the affected solar cells. Assuming that the average backside irradiance is between 10 and 20% of the frontside irradiance, a 20% backside irradiance inhomogeneity will result in a maximum variation of 4% irradiance inhomogeneity over the entire cell.

The effect of local inhomogeneities on the output power of a bifacial solar cell/module can be simulated using SPICE simulations. The results have already been presented in Ref. [13]. The simulations were performed on a standard 120-half-cell PV module in a "butterfly" configuration. If only half of a cell is shaded from the back side, the power loss is negligible, only 0.1%.

Fig. 3 shows the variations in irradiance on the backside of the module during a summer morning in Jaén (37.79° N, −3.78° E). Early in the morning, the sun shines directly on the back of the module. Later, as the sun's azimuth and zenith angles change, the module frame begins to shade the direct sunlight (second and third images in the top row of Fig. 3). Later in the day, the cells only receive the light reflected from the ground and the diffuse light. The amount of the reflected light depends on the ground albedo and the amount of shadow of the module/PV system casts on the ground. The images in the bottom row of Fig. 3 show the movement of the self-shadow during the morning hours that visualizes how strongly reflected light from the ground changes in the morning hours.

2.3. Analytical models

Analytical models are based on site-specific data such as PV system geometry, albedo and surroundings. Key input parameters include global horizontal irradiance (GHI) and diffuse horizontal irradiance (DHI). The backside irradiance is calculated as the sum of diffuse light hitting the backside of the module, reflected light from the ground,

Fig. 1. Mounting conditions of bifacial PV modules/systems. The amount of shading depends largely on the module's ground clearance.

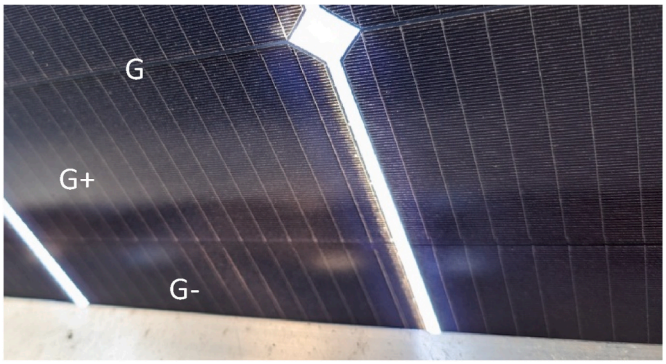

Fig. 2. Example of inhomogeneous backside illumination. Support elements can both shade the cells and create reflections. (For interpretation of the references to colour in this figure legend, the reader is referred to the Web version of this article.)

reflections from surrounding objects and mounting structures, and the direct light that can hit the backside of the module in the summer months. An analytical model can achieve a very high level of accuracy for the site for which it has been modelled, but cannot be easily applied to another site without knowing all the relevant parameters. In general, there are two mathematical approaches: the use of view factors and ray-tracing models.

One of the first models using view factors for reflected light was published by Yusufoglu [6] in 2014. Today, various view factor models are widely used to model backside irradiance. Shoukry et al. is integrating ground reflected light by using view factors including self-shading influences of consecutive rows of modules [25]. Catena et al. [26] upgraded the previously mentioned approach by a better calculation of shaded and unshaded areas. The total area is divided in triangles for a better and faster calculation. Ledesma et al. is calculating backside irradiance by using hypothetical case of infinite and homogeneous Lambertian reflector [27].

One of the most comprehensive analytical models for backside irradiance has been developed by Hansen et al. [10] at Sandia National Laboratories in the USA. The model was developed from data from a small 4 module open-rack PV system by using 10 small reference mini-modules mounted on the back side of the module. The model follows well the shape of the measured back irradiance at different locations on the back side of the module. The same authors also showed that the inhomogeneity of the light on the back of the module varies from a few percent to a few tens of percent in the morning and evening hours. Another model has been published by Marion et al. [28], which also takes into account the reflections from the rear rows of PV modules, using correction factors (derived from the field of view) and angle-of-incidence (AOI) values to estimate the backside irradiance. A simplified model that can be applied to other sites has been developed by Durusoy et al. [29].

Simplified analytical models that consider only the ground reflection are used in the energy performance modelling of bifacial PV systems [6, 30]. Simulation programs such as PVsyst also adopt simplified view factor models, using only albedo and the ground reflectance.

Ray-tracing models require more computing power and a more detailed technical model of the PV system. A detailed review of view factors and ray-tracing models for backside irradiance has recently been published by Ernst et al. [31]. Another ray-tracing model has been published by Louw et al. [32].

In general, analytical models assume an isotropic distribution of the diffuse light and Lambertian ground reflection. As a result, they can

Fig. 3. Irradiance from the back side of a bifacial PV system in the morning hours of May 2024 in Jaén (37.79° N, −3.78° E). (Time is shown in CEST).

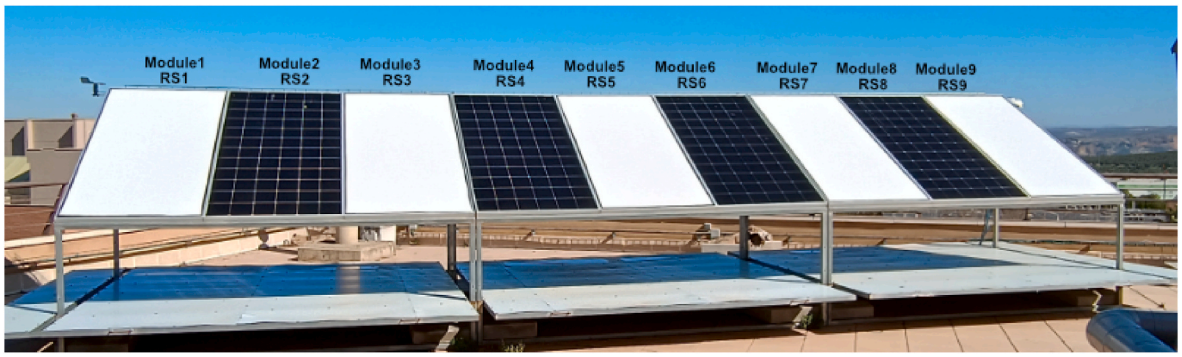

Fig. 4. Test bifacial PV system at the University of Jaén, Spain. Five of the nine PV modules were covered from the front to only absorb light from the back.

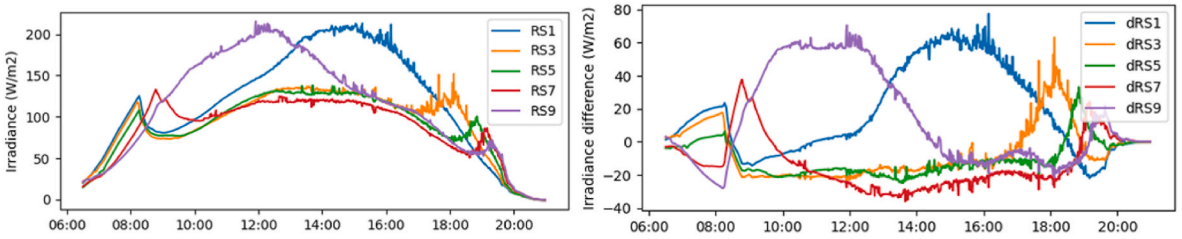

Fig. 5. Backside irradiance measured by modules covered from the front side (left) and deviations from the mean value (right) (module names correspond to the names shown in Fig. 4).

simulate backlighting very accurately on clear days, but are less accurate on cloudy days when the diffuse light is not uniform.

2.4. Empirical models

Empirical models, based on backside irradiance measurements are more versatile than analytical models, but offer less accuracy on an hourly or daily basis. However, they can provide acceptable results for annual simulations, performance evaluation and degradation analyses. They are usually less computationally intensive and can be adapted to any bifacial PV system, regardless of location or mounting conditions. Additionally, empirical models include all local deviations in the irradiance (reflections or shading of the PV modules' supporting structure) since they are trained on measured values.

Currently, all available backside irradiance models are based on view factors or ray tracing techniques. To our knowledge, there is no empirical backside irradiance model in the scientific literature.

3. Development of a new empirical model

This section describes a new empirical model for modelling the backside irradiance of bifacial PV systems. The model has been developed using data from a PV system installed at the University of Jaén, Spain and verified using data from Ljubljana, Slovenia and Neuchâtel, Switzerland.

3.1. Description of the experimental setup

The PV system used in this study for modelling consists of 9 bifacial PV modules, five of which had their front side covered with a white film to block incoming light on the front surface (Fig. 4). These covered modules were used as backside irradiance sensors. Additional instrumentation included a plane-of-array pyranometer, a reference cell and a nearby albedo meter.

3.2. Back irradiance analysis

Using whole PV modules as irradiance sensors has some advantages over small area reference solar cells or pyranometers. The integrated irradiance measured by the module's short-circuit current better reflects the actual energy it would receive at its location, whereas reference cells or pyranometers only provide spot measurements, so their value may differ from the actual amount of energy a module receives.

Fig. 5 illustrates the measured irradiance values (left side) and the deviations from the mean value. As expected, the modules at the edges receive higher irradiance in the morning or evening hours (RS9 in the

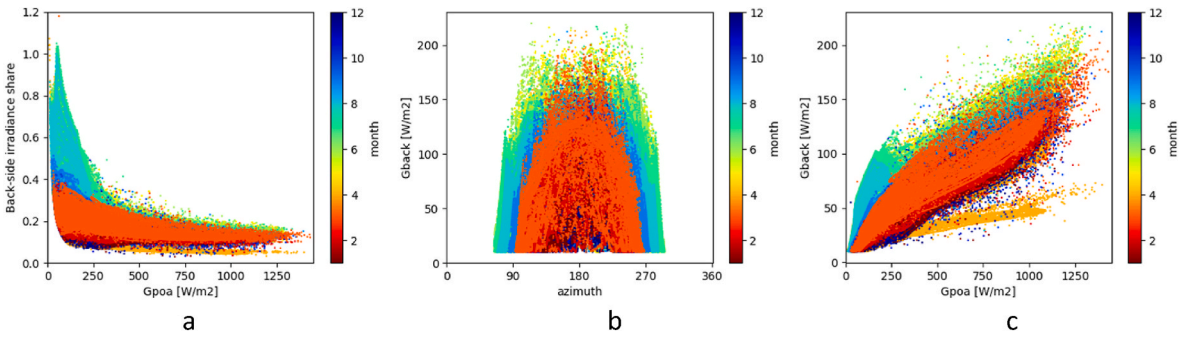

Fig. 6. Backside irradiance share versus plane-of-array irradiance (a), backside irradiance versus solar azimuth (b) and plane-of-array irradiance (c) in Jaén.

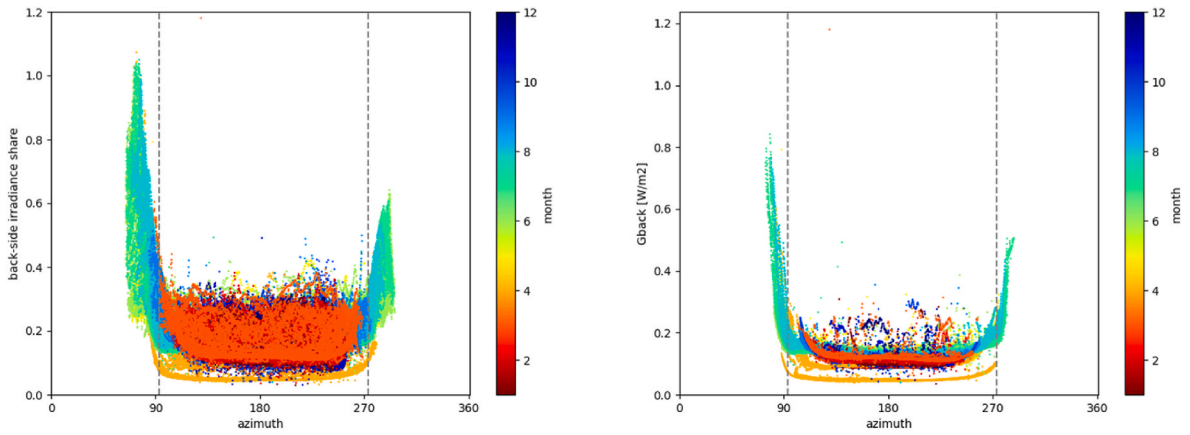

Fig. 7. Backside irradiance share versus solar azimuth over the whole year (left) and for clear-sky days (right). Colour represent the month. Values for month of April deviate due to maintenance work on the floor reflector. The vertical dashed lines present when solar azimuth is perpendicular to the PV system azimuth. (For interpretation of the references to colour in this figure legend, the reader is referred to the Web version of this article.)

morning hours at the eastern end of the string; RS1 in the evening hours at the western edge of the string). This is due to the higher ground reflection in the area where the shadow cast by the modules is not present. Due to an uneven ground albedo (with a highly reflective ground surface below the modules) and a low sun position, the modules on the east side received higher irradiance values in the early morning hours than the modules on the west side of the string (and vice versa in the evening hours). The central modules exhibit more consistent irradiance throughout the day. Morning and evening peaks in summer (before 9 a.m. and after 7 p.m.) are caused by the direct sunlight hitting the module from behind as the sun shines from the "back" of the module when the difference between the sun's azimuth angle and the module orientation is greater than 90°.

The backside irradiance is analysed at the back of the central module of the PV array (module RS5 in Fig. 4). Fig. 6a shows the calculated backside irradiance share (G_{back_share}) relative to the plane-of-array irradiance G_{poa} at the centre of the PV array. G_{back_share} is defined as G_{back} divided by G_{poa}. The colour represents the month (referenced as in-plane rear-side irradiance ratio in IEC 61724-1 standard [33]). At low global irradiance levels, the backside share is high but at $G_{poa} > 500$ W/m^2 it is mostly below 20% in Jaén. This is mainly due to illumination from the back in morning and evening hours (in summer), and as also under cloudy skies, when the ratio depends mainly on the sky view and ground view factors.

Fig. 6b and c shows that backside irradiance never exceeds 200 W/m^2. The values in April (Fig. 6c) are low due to the maintenance work on the ground reflector.

The most interesting plot is the backside irradiance share versus the solar azimuth angle as shown in Fig. 7 for all data and clear-sky data (DHI < 0.2 * GHI), respectively. The backside irradiance share remains almost constant when the sun shines from the front but deviates significantly when the sun is shining from behind. Sun's azimuth angle is counted from north (East: 90°, south:180°, west: 270°).

The shape of the measured backside irradiance versus the solar azimuth can be modelled with an exponential function (with a shape of an inverse Gaussian distribution function), which varies on a monthly basis:

$$G_{back\_share} = y_0 + a \cdot e^{-0.5 \cdot \left(\frac{|az - az_0|}{b}\right)^c} \quad \text{Eq. 1}$$

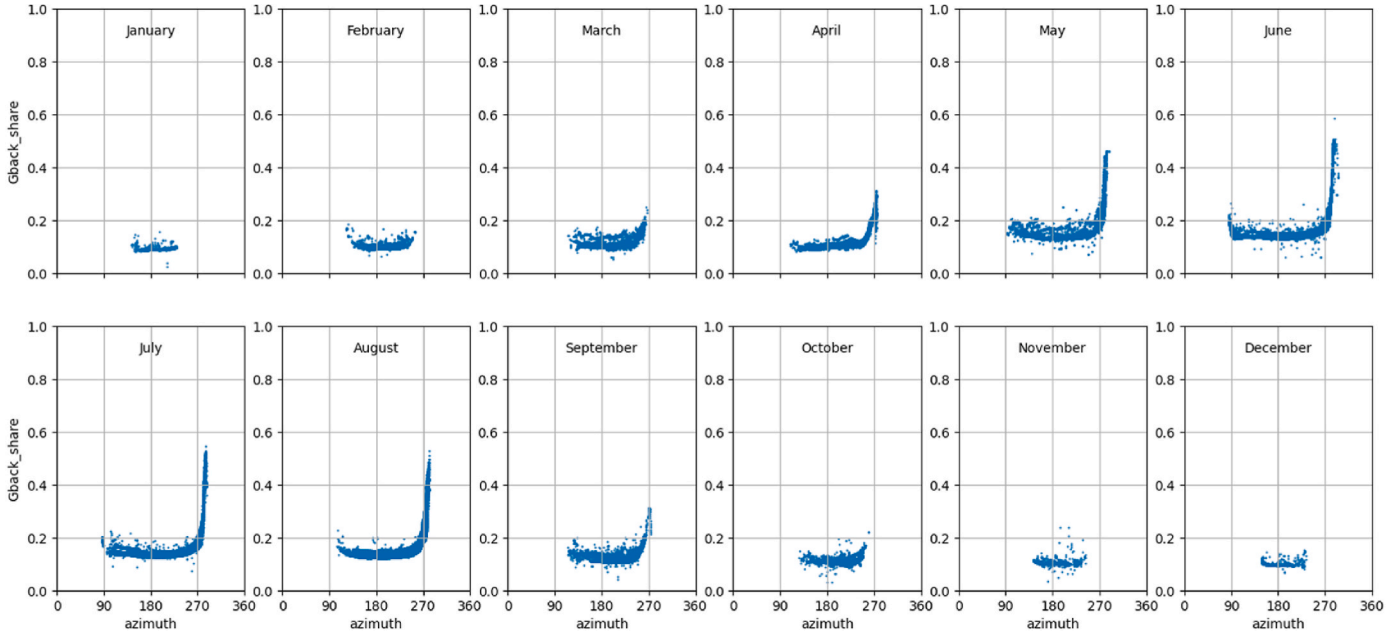

Fig. 8. Monthly backside irradiance shares at clear skies (DHI/GHI < 0.5).

Table 1
Parameters of Gaussian function.

coefficient	value	comment
a	−800	tail slope
b	130–170	width
c	15	width and "sharpness"
az_0	184	azimuth shift (183–184 for Jaén)
y_0	800.14	|a|+ effective albedo

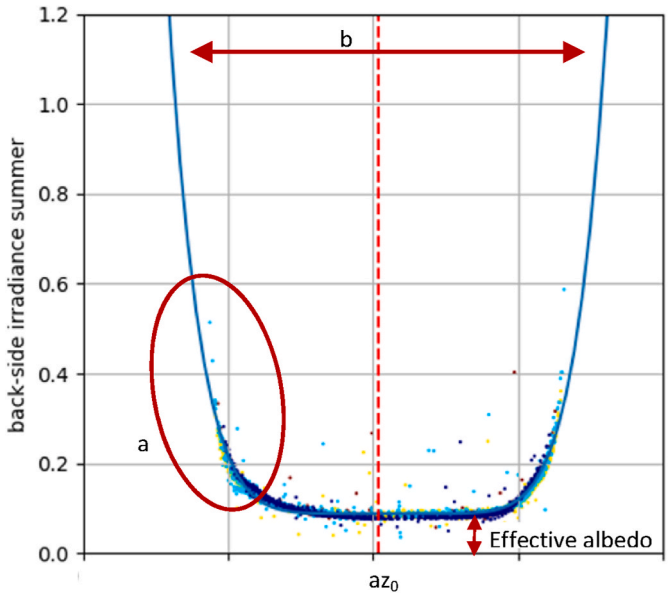

Fig. 9. Gaussian function.

where az and az_0 are the solar azimuth angle and the azimuth angle of the PV system, respectively. Fig. 8 illustrates the clear sky G_{back_share} plotted against the solar azimuth angles.

The average values of the coefficients a, b, c, az_0 and y_0 are summarized in Table 1. Their physical interpretations are illustrated in Fig. 9. The coefficient a represents the slope of the tail in the morning and evening hours and an average value can be used for all months. Coefficient b influences the width of the Gaussian function "well" and varies with regard to the length of the year. Similarly, the coefficient c influences the width of the function as well as the "sharpness" at the edges. The az_0 coefficient is related to the geographical location of the site. It represents the position of the sun at noon. Jaén is located at W 3.8° thus $az_0 = 184$. The constant backside irradiance share during the day is denoted as effective albedo in this article. Finally, y_0 is the sum of

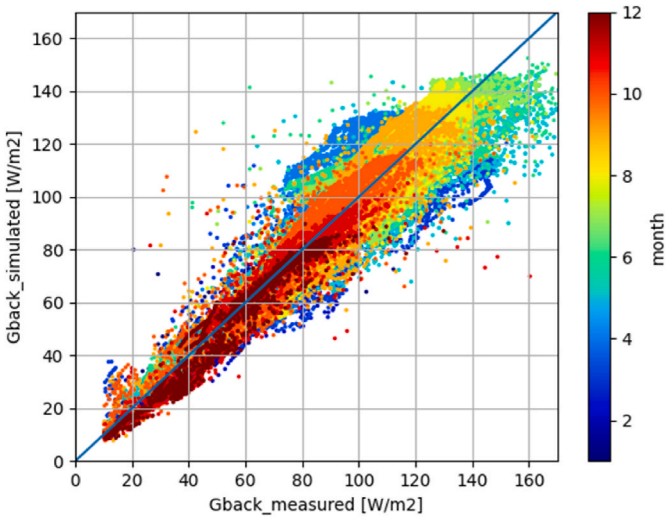

Fig. 11. Simulated versus measured backside irradiance over one year in Jaén. (Colour represents month). (For interpretation of the references to colour in this figure legend, the reader is referred to the Web version of this article.)

the effective albedo and the absolute value of the coefficient a.

The initial parameters of the Gaussian function are obtained by fitting the measured G_{back_share} values for clear-sky data for each month. The parameters b and y_0 show a monthly dependence, while for the parameters a, c, and az_0 an annual average is used. The parameter b is directly related to the length of the day, while the y_0 is related to the effective albedo. A detailed comparison of the solar azimuth angle at sunrise and factor b shows a perfect correlation, as shown in Fig. 10a. The effective albedo value can also vary over the year and can be modelled with a 4th order polynomial function as shown in Fig. 10b. In addition to monthly changes, effective albedo changes also with the share of the diffuse light (see Fig. 7). On cloudy days, the effective albedo is almost twice as high as on clear days (see Fig. 7), therefore the effective albedo is additionally corrected by the share of the diffuse light.

The simulated backside irradiance compared to the measured one is shown in Fig. 11, where colour represents the month of the year.

The simulations show a fairly good agreement with the measured values. The deviations of the simulations at lower values (around 50 W/m^2), which are mainly visible in summer, are due to reflections and shading in the morning and evening hours. The scatter at the higher values is mainly due to the daily changes in the effective albedo values. In winter time, when the zenith angle of the sun is high, the ground below the PV modules is fully illuminated, while in the summer, when the zenith angle of the sun is lower, the shadow cast of the PV modules

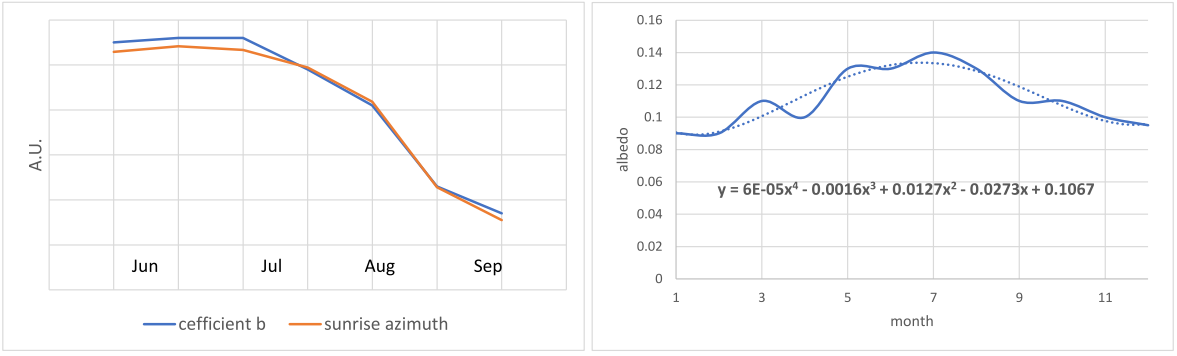

a b

Fig. 10. Correlation between parameter b and solar azimuth at sunrise (left) and monthly effective albedo (measured and interpolated - right).

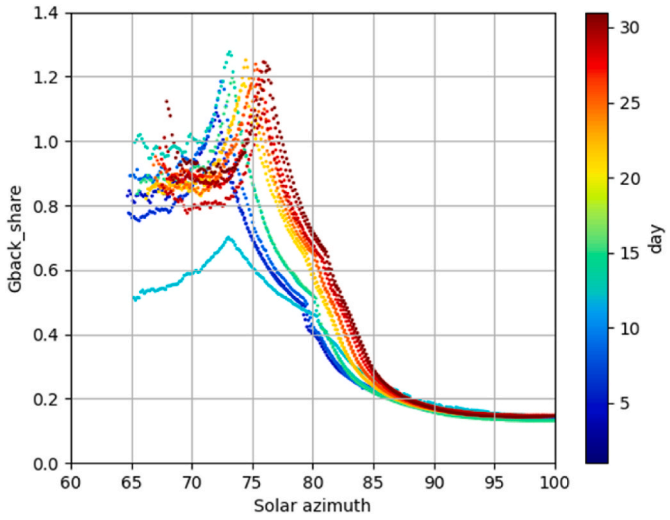

Fig. 12. Backside irradiance share versus solar azimuth in the morning hours of July.

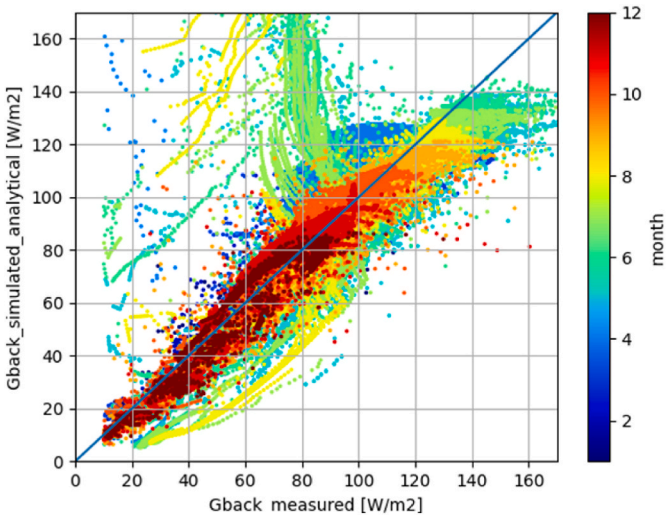

Fig. 14. Annual simulated vs. measured backside irradiance with analytical model on a clear-sky summer day in Jáen.

affects the proportion of the illuminated ground area and therefore the effective albedo value. However, the direct light can be reflected directly onto the back side of the module, which leads to an increase of the effective albedo.

The modelling challenges in the morning and evening hours in summer can be better observed under clear sky conditions. Fig. 12 shows the backside irradiance as a function of the azimuth angle of the sun in the month of July. The colour represents the day. The peak is when the sun starts to shine on the front side of the module (AOI <85°). There is also a break in the curve between solar azimuth angles of about 80°. We believe this is caused by two reasons. First, the shadow of the module frame begins to spread across the back side of the module (see photos in Fig. 3), and second, the angular dependence of the module becomes constant around this point [34]. There are also some 'outliers' in the early hours at lower azimuths. These are caused by reflections of light from the attica. These phenomena cannot be modelled by the single Gaussian function (Eq. (1)), but do affect the accuracy of the model.

3.3. Verification and comparison with an analytical model

Backside irradiance modelling presents significant challenges, and evaluating the quality of the results is not straightforward. To our knowledge, no empirical models have been published to date, therefore, in order to validate our approach, the results were compared with an analytical model similar to that of Sandia Lab [10].

The model developed calculates the solar angles on an hourly basis, separating the incident irradiance into direct and diffuse components. Reflections are computed for both shaded and unshaded areas. In shaded regions, a Lambertian reflection of diffuse light is assumed, while in unshaded areas, both diffuse and direct light reflections are considered.

Fig. 13 shows a clear-sky daily profile comparing measured and Fig. 14 modelled backside irradiance. While the model achieves an almost perfect fit when the sun is high, deviations are more pronounced during morning and evening hours, when sunlight enters from behind the module. The main problem is before the sun's azimuth becomes perpendicular to the module orientation (marked with red circle in Fig. 13) and the module frame starts to shade the back of the module. The annual simulation of G_{back} is shown in Fig. 14. There are many outliers in the morning and evening hours. There are also worse results in the winter months when diffuse light plays a major role. The diffuse light is treated isotropically.

The analytical and empirical results are very similar when the outliers or simulation results are omitted for solar azimuths below 90° or above 270°. Fig. 15 shows the simulation root mean square (RMS) error with regard to the measured values of both methods (omitting data from morning and evening hours in analytical model).

The developed empirical model was further validated in two additional locations in Europe: Neuchâtel, Switzerland and Ljubljana, Slovenia. Both sites are equipped with G_{poa} and G_{back} measurements, and the PV system is located on a gravel-covered roof. The PV modules in Ljubljana are approximately 1 m above the ground, while in Neuchâtel they are mounted in single-module row in a landscape orientation directly above the ground. The validation was performed at the module level. However, in all cases, the modules were mounted in a row, which

Fig. 13. Simulated vs. measured backside irradiance with analytical model on a clear-sky summer day in Jáen.

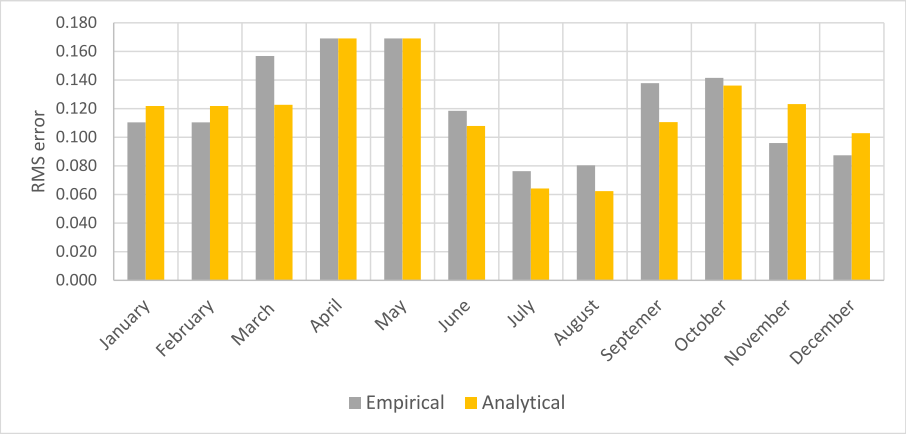

Fig. 15. Monthly RMS error of analytical and empirical model in Jáen.

means that their response is comparable to that of a PV system row. At one location (Neuchâtel), there were also rows behind the observed one, as in a typical free-standing PV system, meaning that reflections from the next row were also considered.

Fig. 16 compares simulated G_{back} values to measured data from these locations. The results were generally consistent, although absolute values in Ljubljana were approximately half of those in Jaén and values in Neuchâtel were almost an order of magnitude lower. The values in Neuchâtel are attributed to its specific installation conditions (small ground clearance).

4. Discussion

Modelling backside irradiance in PV systems is a complex and system-specific process. Therefore, there is no common, globally valid simple model. Existing available models are based on the geometry of the sun and the PV system, or at least on sky view factors. In contrast, our new model uses an empirical equation to simulate the backside irradiance. Both approaches can yield good results but the questions arise whether an accurate backside irradiance is essential when calculating the PV system performance indicators.

We applied the simulated backside irradiance to our recently developed DDPRbifi model [13] and compared the results obtained against measured backside irradiance and a fixed proportion of the backside irradiance (average annual value). Fig. 17 shows the simulated power output of a PV module using (a) measured irradiance, (b) a fixed share, (c) the empirical backside irradiance model, and (d) the analytical backside irradiance model. All results are almost the same regardless of the G_{back} used. Except the results with the analytical model deviate from the measured one.

Although the results across the three methods are similar on an annual basis, the simulation error on an hourly basis is more variable. A clear-sky daily simulation profile for all three cases (from Fig. 17) is shown in Fig. 18. Both simulated values of G_{back} slightly overestimate the backside irradiance and thus module output power around midday and underestimate it in the morning and evening hours (Fig. 18 bottom).

These findings indicate that for the annual performance assessment it may be sufficient to calculate the backside irradiance using only a constant share of the G_{poa} irradiance or by applying a sky view factor. For an accurate daily or instantaneous simulation, analytical models with knowledge of all PV system parameters and ground albedo are required. However, for annual power predictions, the backside irradiance is not a critical parameter, at least for common sites in Europe or sites at similar latitudes. Sites with high albedo values and therefore a higher G_{back} share may require different considerations.

5. Conclusion

Modelling complex parameters such as solar irradiance is always challenging. Many assumptions and simplifications must be made to create a relatively simple and reliable model. Backside irradiance introduces additional parameters, such as reflections and shading, to the equation, making the problem even more complex. In this paper, we present the issues associated with backside irradiance models and

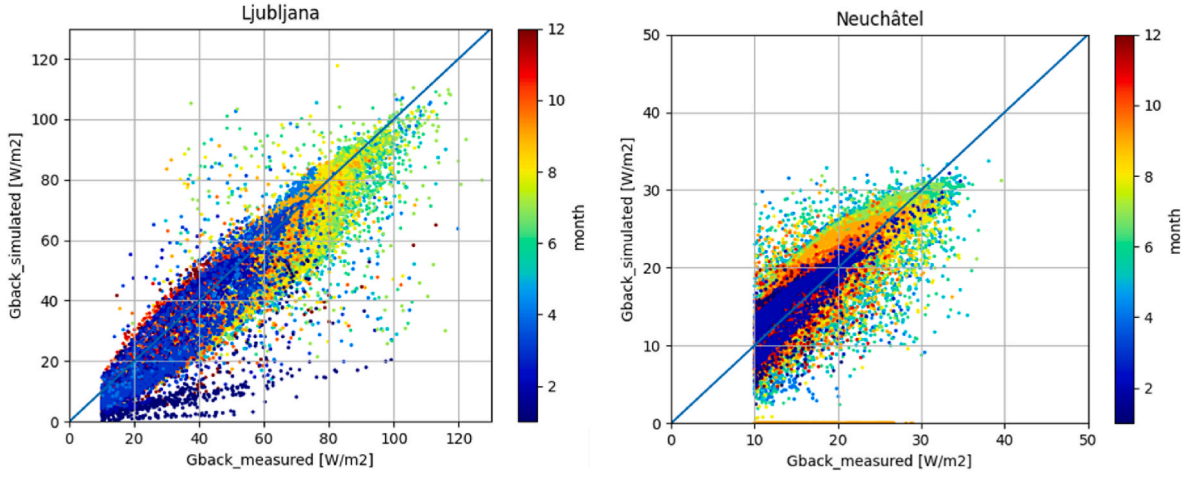

Fig. 16. Backside irradiation modelling results in Ljubljana (left) and Neuchâtel (right). The simulation period is one year.

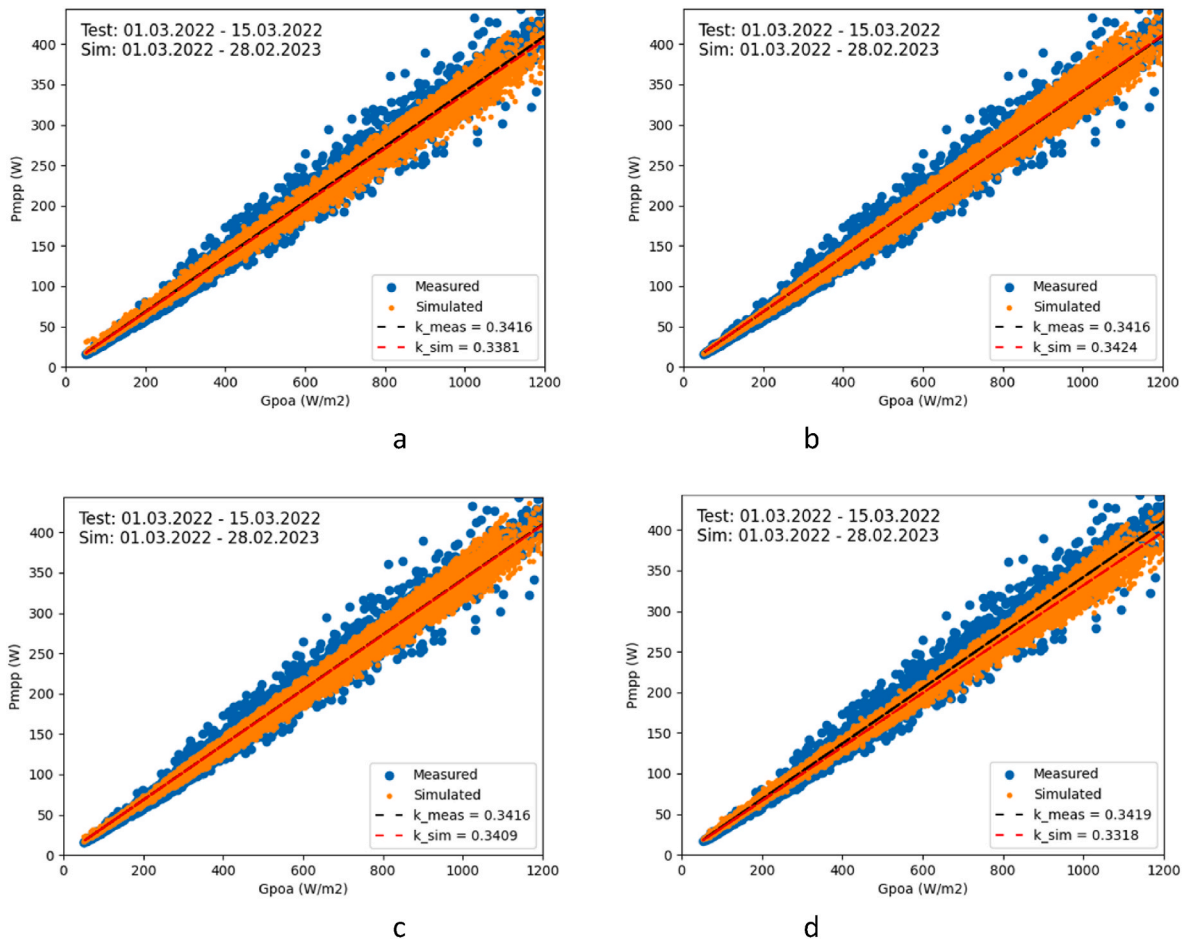

Fig. 17. Simulated and measured power output of a PV module in Ljubljana (a – with measured backside irradiance, b – with fixed backside irradiance share, c – using empirical backside irradiance model, d – using analytical backside irradiance model).

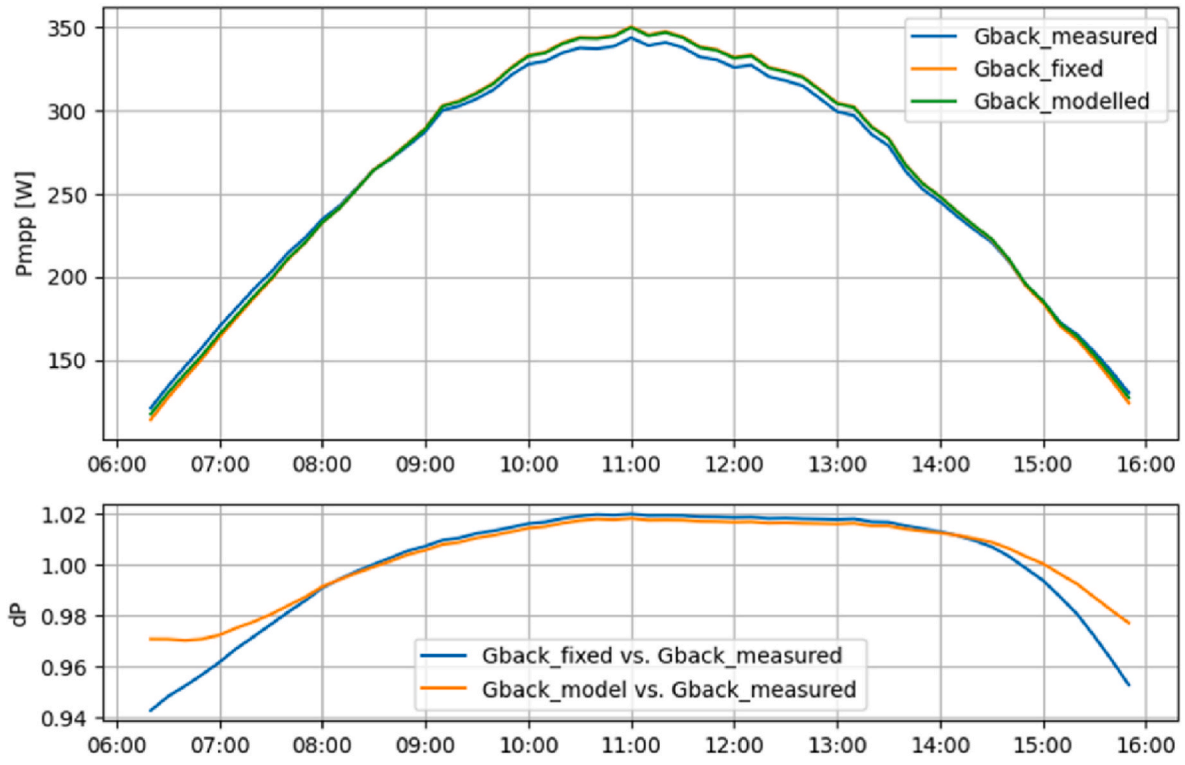

Fig. 18. Simulated and measured module output power on a clear-sky day (top) and relative difference to the results when measure G_{back} were used (bottom).

provide an overview of existing models, including a new empirical model. Ultimately, we cannot provide a definitive answer as to which model is superior. The majority of available models use view factors or exact PV system geometry information. This can improve model accuracy if the data is available. However, if simulations are performed on an unknown PV system for which only basic data is available (e.g. the orientation and inclination angle of the modules and the distance between rows), this can lead to higher uncertainty. Furthermore, analytical models cannot consider local phenomena such as reflections and shading due to railings. In contrast, empirical models do not require knowledge of the geometry; however, they require information on measured backside irradiance values for the training period. Measured data can more accurately represent the situation on the back of the modules.

Both analytical and empirical models are usually created for one location in the system, or multiple calculations (and measurements in the case of empirical models) must be carried out. Our study showed that the new empirical model can compete with analytical models, with the advantage of not requiring detailed knowledge of PV system geometry. However, it does require initial training with measured backside irradiance data.

The new empirical model simulates the backside irradiance by determining its share relative to G_{poa}. The share of the back irradiance in the total irradiance received by a bifacial module is generally consistent throughout the day, with deviations in the morning and evening hours in summer when the sun shines from behind. Our new empirical model simulates the backside irradiance share as a ratio of the back to front irradiance with respect to the solar azimuth. The share is modelled by an exponential equation of inverse Gaussian distribution shape with the parameters derived from the measured data in the training period.

The validation of the model was performed on PV modules at three different locations in Europe. Since the model was derived from data in the middle of the row of PV modules, the results are valid also for PV systems with long rows where the backside conditions do not change much. The situation at the edge modules is different and will be analysed in our future work.

Performance calculations for PV systems show that precise backside irradiance modelling is often unnecessary. Since the share of the backside irradiance is usually in the range of 10%, annually, a simple value of a backside irradiance share over the whole year is sufficient for an annual performance assessment and is also acceptable on an hourly level for most common sites in Europe or similar latitudes. Sites with high albedo may require additional analysis to account for their specific conditions.

CRediT authorship contribution statement

Kristijan Brecl: Writing – original draft, Validation, Software, Methodology, Investigation, Formal analysis, Conceptualization. **Emilio Muñoz Cerón:** Writing – review & editing, Supervision, Project administration. **Juan de la Casa Higueras:** Writing – review & editing, Project administration. **Marko Topič:** Writing – review & editing, Supervision, Project administration, Funding acquisition.

Declaration of competing interest

The authors declare that they have no known competing financial interests or personal relationships that could have appeared to influence the work reported in this paper.

Acknowledgement

The Authors acknowledge the financial support of the Slovenian Research Agency (Research Programme P2-0415). This work has been possible also thanks to the project "Demo_BI-FV: Development of Advanced Models for the characterization of bifacial photovoltaic systems (PID2021-124161OB-I00)" funded by the Spanish Ministry of Science and the State Innovation Agency within the European Regional Development Fund (MCIN/AEI/10.13039/501100011033/FEDER, UE).

References

[1] ITRPV, International Technology Roadmap for Photovoltaic, fifteenth ed., ITRPV, Apr. 2024 [Online]. Available: itrpv.net/Reports/Downloads/. (Accessed 25 July 2024).
[2] J.P. Singh, S. Guo, I.M. Peters, A.G. Aberle, T.M. Walsh, Comparison of glass/glass and glass/backsheet PV modules using bifacial silicon solar cells, IEEE J. Photovoltaics 5 (3) (May 2015) 783–791, https://doi.org/10.1109/JPHOTOV.2015.2405756.
[3] Internationale Elektrotechnische Kommission, Photovoltaic devices - part 1-2: measurement of current-voltage characteristics of bifacial photovoltaic (PV) devices [Online]. Available: https://webstore.iec.ch/en/publication/34357. (Accessed 25 July 2024).
[4] M.R. Vogt, G. Pilis, M. Zeman, R. Santbergen, O. Isabella, Developing an energy rating for bifacial photovoltaic modules, Prog. Photovoltaics Res. Appl. (Feb. 2023), https://doi.org/10.1002/pip.3678 pip.3678.
[5] Photovoltaic *(PV) module performance testing and energy rating. Part 3: standard reference climatic profiles*, edition 1.0, 2018-08, in: Internationale Elektrotechnische Kommission (Ed.), International Standard/International Electrotechnical Commission, IEC, Geneva, 2018, pp. 61853–61854.
[6] U.A. Yusufoglu, et al., Simulation of energy production by bifacial modules with revision of ground reflection, Energy Proc. 55 (Jan. 2014) 389–395, https://doi.org/10.1016/j.egypro.2014.08.111.
[7] G.J.M. Janssen, B.B. Van Aken, A.J. Carr, A.A. Mewe, Outdoor performance of bifacial modules by measurements and modelling, Energy Proc. 77 (Aug. 2015) 364–373, https://doi.org/10.1016/j.egypro.2015.07.051.
[8] M. Chiodetti, Bifacial PV Plants: Performance Model Development and Optimization of Their Configuration, KTH ROYAL INSTITUTE OF TECHNOLOGY, Stockholm, 2015 [Online]. Available: https://urn.kb.se/resolve?urn=urn:nbn:se:kth:diva-172516. (Accessed 3 October 2023).
[9] S. Wang, et al., Bifacial photovoltaic systems energy yield modelling, Energy Proc. 77 (Aug. 2015) 428–433, https://doi.org/10.1016/j.egypro.2015.07.060.
[10] C. Hansen, D. Riley, C. Deline, F. Toor, J. Stein, A detailed performance model for bifacial PV modules, Sandia Natl. Lab. (2017), 33rd Eur. Photovolt. Sol. Energy Conf. Exhib. 2395-2400, doi:10.4229/EUPVSEC20172017-6BV.2.35.
[11] C.E. Valdivia, et al., Bifacial photovoltaic module energy yield calculation and analysis, in: 2017 IEEE 44th Photovoltaic Specialist Conference (PVSC), Jun. 2017, pp. 1094–1099, https://doi.org/10.1109/PVSC.2017.8366206.
[12] S. Bouchakour, D. Valencia-Caballero, A. Luna, E. Roman, E.A.K. Boudjelthia, P. Rodríguez, Modelling and simulation of bifacial PV production using monofacial electrical models, Energies 14 (14) (Jan. 2021), https://doi.org/10.3390/en14144224. Art. no. 14.
[13] K. Brecl, M. Bokalič, A. Faes, M. Topič, An accurate bifacial PV module energy performance model using a direct-diffuse power rating model, Appl. Energy 382 (Mar. 2025) 125310, https://doi.org/10.1016/j.apenergy.2025.125310.
[14] ASHRAE Handbook of Fundamentals, Altlanta, GA, American Society of Heating, Refrigerating and Air-Conditioning Engineers, Inc., 1972.
[15] R. Bird, C. Riordan, and S. E. R. Institute, "Simple Solar Spectral Model for Direct and Diffuse Irradiance on Horizontal and Tilted Planes at the Earth's Surface for Cloudless Atmospheres".
[16] P. Ineichen, A broadband simplified version of the solis clear sky model, Sol. Energy 82 (8) (Aug. 2008) 758–762, https://doi.org/10.1016/j.solener.2008.02.009.
[17] C.A. Gueymard, Clear-sky irradiance predictions for solar resource mapping and large-scale applications: improved validation methodology and detailed performance analysis of 18 broadband radiative models, Sol. Energy 86 (8) (Aug. 2012), https://doi.org/10.1016/j.solener.2011.11.011. Art. no. 8.
[18] F. Kasten, G. Czeplak, Solar and terrestrial radiation dependent on the amount and type of cloud, Sol. Energy 24 (2) (Jan. 1980) 177–189, https://doi.org/10.1016/0038-092X(80)90391-6.
[19] V. Badescu, A new kind of cloudy sky model to compute instantaneous values of diffuse and global solar irradiance, Theor. Appl. Climatol. 72 (1–2) (May 2002) 127–136, https://doi.org/10.1007/s007040200017.
[20] U. Pfeifroth, et al., Surface Radiation Data Set - heliosat (SARAH) - edition 2, Satell. Appl. Fac. Climate Monit. (CM SAF) (2017), https://doi.org/10.5676/EUM_SAF_CM/SARAH/V002, 7.1 TiB, Jun. 13.
[21] K.-G. Karlsson, et al., CLARA-A2: the second edition of the CM SAF cloud and radiation data record from 34 years of global AVHRR data, Atmos. Chem. Phys. 17 (9) (May 2017) 5809–5828, https://doi.org/10.5194/acp-17-5809-2017.
[22] Copernicus Climate Change Service (C3S), ERA5: fifth generation of ECMWF atmospheric reanalyses of the global climate. Copernicus Climate Change Service Climate Data Store (CDS), Copernicus Climate Change Service (C3S). [Online] Accessed: January. 4, 2022. Available: https://cds.climate.copernicus.eu/cdsapp#!/home.
[23] R. Perez, P. Ineichen, R. Seals, J. Michalsky, R. Stewart, Modeling daylight availability and irradiance components from direct and global irradiance, Sol. Energy 44 (5) (Jan. 1990), https://doi.org/10.1016/0038-092X(90)90055-H. Art. no. 5.

[24] J.E. Hay, Calculating solar radiation for inclined surfaces: practical approaches, Renew. Energy 3 (4–5) (Jun. 1993) 373–380, https://doi.org/10.1016/0960-1481(93)90104-O.
[25] I. Shoukry, J. Libal, R. Kopecek, E. Wefringhaus, J. Werner, Modelling of bifacial gain for stand-alone and in-field installed bifacial PV modules, Energy Proc. 92 (Aug. 2016) 600–608, https://doi.org/10.1016/j.egypro.2016.07.025.
[26] M. Catena, I. Cascone, M. Carbone, Performance estimation of bifacial PV modules: a simulation approach through both physical and semi-empirical math models and its validation using real bifacial plant data, in: 33rd Eur. Photovolt. Sol. Energy Conf. Exhib, 2017, pp. 1968–1972, https://doi.org/10.4229/EUPVSEC20172017-6CO.13.4, p. 5 pages, 4642 kb.
[27] J.R. Ledesma, et al., A simulation model of the irradiation and energy yield of large bifacial photovoltaic plants, Sol. Energy 206 (Aug. 2020) 522–538, https://doi.org/10.1016/j.solener.2020.05.108.
[28] B. Marion, et al., A practical irradiance model for bifacial PV modules, in: 2017 IEEE 44th Photovoltaic Specialist Conference (PVSC), IEEE, Washington, DC, Jun. 2017, pp. 1537–1542, https://doi.org/10.1109/PVSC.2017.8366263.
[29] B. Durusoy, T. Ozden, B.G. Akinoglu, Solar irradiation on the rear surface of bifacial solar modules: a modeling approach, Sci. Rep. 10 (1) (Aug. 2020) 13300, https://doi.org/10.1038/s41598-020-70235-3.
[30] F.R. Galluzzo, A. Canino, C. Gerardi, S.A. Lombardo, A new model for predicting bifacial PV modules performance: first validation results, in: 2019 IEEE 46th Photovoltaic Specialists Conference (PVSC), Jun. 2019, pp. 1293–1297, https://doi.org/10.1109/PVSC40753.2019.8980925.
[31] M. Ernst, C.-A. Asselineau, P. Tillmann, K. Jäger, C. Becker, Modelling bifacial irradiance – step-By-Step comparison and validation of view factor and ray tracing models, Appl. Energy 369 (Sep. 2024) 123574, https://doi.org/10.1016/j.apenergy.2024.123574.
[32] J.A. Louw, A.J. Rix, Irradiance modelling for bi-facial PV modules using the ray tracing technique, in: 2019 Southern African Universities Power Engineering Conference/Robotics and Mechatronics/Pattern Recognition Association of South Africa (SAUPEC/RobMech/PRASA), Jan. 2019, pp. 383–388, https://doi.org/10.1109/RoboMech.2019.8704817.
[33] Photovoltaic system performance - part 1: monitoring, in: Internationale Elektrotechnische Kommission (Ed.), International Standard/International Electrotechnical Commission, second ed., IEC, Geneva, 2021 no. 61724–1, 2021.
[34] N. Martin, J.M. Ruiz, Calculation of the PV modules angular losses under field conditions by means of an analytical model, Sol. Energy Mater. Sol. Cells 70 (1) (Dec. 2001), https://doi.org/10.1016/S0927-0248(00)00408-6. Art. no. 1.